Far-Field Seismic Radiation and Its Dependence upon the Dynamic Fracture Process

Sci. Rep. Tôhoku Univ., Ser. 5, Geophysics, Vol. 24, No. 3, pp. 73-87, 1977.

Far-Field Seismic Radiation and Its Dependence upon the Dynamic Fracture Process

TETSU MASUDA, SHIGEKI HORIUCHI and AKIO TAKAGI

Aobayama Seismological Observatory, Faculty of Science
Tohoku University, Sendai 980, Japan

(Received May 28, 1977)

Abstract: We study the dynamic radiation field of seismic waves applying the dynamic solutions for antiplane strain shear cracks obtained in a previous paper to circular faults as the source function of slip. The dependence of seismic radiations upon the dynamic fracture process at the source is investigated through the physical conditions on the fault. It is shown that the P-wave corner frequencies are systematically larger than the S-wave corner frequencies. The ratio is about 1.70 at higher angles measured from the normal to the fault, which is in good accordance with the observed data for small earthquakes. This is considered due to the dynamic characteristics of the source process that slip on the fault continues after the rupture propagation stops and that slip at the edge of the fault is nearly represented as a step function. Since slip on the fault continues after the fault stops expanding, the radiated seismic waves have longer predominant periods than predicted in the previous studies for the same source dimension. This implies that our model estimates the source dimensions at smaller values than those to be estimated according to other source models. Smaller estimates of the source dimensions lead to larger stress drop to be estimated. Our study suggests that for the proper estimates of the stress drop associated with earthquakes the model used should be such as satisfies the physical requirements of the dynamic conditions for the fracturing process, and that necessary may be the sufficient examination of the model in terms of the physical process at the source of earthquakes.

1. Introduction

In recent years, partly owing to the development of the observing system which brings qualified seismic data and partly through the accumulative knowledge about the seismic source mechanism, it has been possible to discuss the seismic source process in detail. The study of the seismic source process is considered to be a promising approach to the investigation of the physical state of material within the Earth. It is required that the estimates of the physical state of material at the focus based upon the seismic data should be a reasonable derivation from the physical standpoint. In this sense, it is important to study the characteristics of the seismic radiation fields in relation to the physical process in the source region.

It has been shown that seismic radiations are generated by shear faulting at the focus. Dislocation models have successfully been used in predicting seismic radiations in the near- and far-fields (Haskell, 1964, 1969; Savage, 1966; Aki, 1968) and in the analyses of long-period seismic waves (Brune and Allen, 1967; Wyss and Brune, 1968; Izutani, 1974). Unfortunately these models have arbitrarily assumed that the

dislocation motion occurs as a simple function in time and in space. Much of an effort has been made to eliminate the arbitrariness in specifying the dislocation time function. Archambeau (1968) and Burridge (1969) have regarded the seismic source process as a relaxation of the initial pre-stress in the source region. Brune (1970) has derived a theoretical representation of the shear wave spectra in the near-and far-fields considering that the time function is directly related to the effective stress available for the acceleration of the two sides of the fault. A theoretical P-wave spectrum has been given on a similar basis by Hanks and Wyss (1972) and Trifunac (1972). These models have predicted the higher value of the P-wave corner frequency than the S-wave corner frequency. Brune's model has widely been used in the studies of seismic waves to estimate the source parameters of earthquakes (Wyss and Hanks, 1972; Thatcher and Hanks, 1973). His derivation, however, seems largely intuitive. The effect of the rupture propagation is not sufficiently examined, and the spatial variation of the dislocation time function not accounted for. Sato and Hirasawa (1973), on the other hand, have proposed a source model which counts in the rupture propagation and the spatial variation of the dislocation function. They have specified the dislocation time function on the assumption that the stress is held in static equilibrium at each moment during rupture. Their model also gives the higher corner frequencies of P waves than those of S waves. In their model, the rupture velocity is arbitrary as far as it is subsonic. The validity of their assumption of static equilibrium of the stress in the dynamic problem is much dependent upon the value of the rupture velocity. It has been discussed that their specification of the dislocation time function is justified from the physical standpoint when the rupture velocity is rather low. (Masuda et al., 1977). Recently Madariaga (1976) has studied the dynamic process of expanding circular faults and has obtained remarkable results about the dynamic features of seismic radiation fields. His model, however, has arabitrairly assumed the value of the rupture velocity independent of stress conditions on the fault. The difficulty in modelling the seismic source process may be the specification of the dislocation time function and the rupture velocity in relation to certain physical conditions on the fault.

Recently the seismic source process have been studied in detail through the relation between the spectral parameters of seismic waves and the source parameters. Especially, the estimation of the stress release associated with earthquakes has been an important problem. A proper estimation of the stress release during an earthquake requires that the source dimension should be estimated properly. For a proper estimation of source parameters, the model used should be founded on the physical basis, the dislocation time function and the rupture velocity being specified so as to reflect the physical conditions in the source region. They should be derived as solutions to certain physical conditions but should not be given either arbitrarily nor independently.

Burridge (1975) has shown that the P-wave corner frequencies are higher than the S-wave corner frequencies for most of the observation points from the application of a self-similar solution of circular shear cracks propagating at the P-wave velocity to the source time function. Savage (1972) has studied the characteristics of the far-field radia-

tion spectra for a long thin fault model of Haskell (1964). The results show that the P-wave corner frequencies are no more than the S-wave corner frequencies. Savage (1974) has generalized the Haskell fault model to a circular fault to show that the S-wave corner frequencies are on the average higher than the P-wave corner frequencies. Dahlen (1974) has also obtained similar results about the relation between the P- and the S-wave corner frequencies for self-similar shear cracks expanding at a velocity lower than the Rayleigh wave velocity. The difference in the relation between the P- and the S-wave corner frequencies in these literatures is considered due to the difference in the dynamic process of fault slip, which is to result from the physical conditions at the source. Discussions of the relation between the P- and the S-wave corner frequencies require the sufficient investigation of the dynamic features of the fracture process at the source under the physical conditions to be considered.

We have studied in a previous paper the dynamic fracture process in the presence of the static and the dynamic frictions as modelling the source process of small earthquakes. The solutions are obtained to physical conditions with no assumptions but the stress boundary conditions given on the fault surface. The solutions are considered to represent the dynamic motion of slip on the fault. In this paper, we investigate the characteristics of seismic radiations applying the solutions previously obtained for the antiplane strain shear cracks to circular faults as the source time function, and the effects of the dynamic fracture process on the seismic radiation field are discussed.

2. Dislocation time function

We have recently studied the dynamic fracture process for the two-dimensional antiplane strain shear cracks in the presence of the static and the dynamic frictions as medelling the source process of small earthquakes (Masuda et al., 1977). Only the stress boundary conditions given on the fault surface have been assumed, but no other assumptions being made. Note that the rupture velocity has not been given independently but has been derived as a consequent result to the stress conditions. It is considered, as concerns the fracture process during an earthquake, that frictional sliding is more likely at the source and that our solutions well represent the slip motion on the fault. The viscous term of the dynamic friction has been counted in as a mechanism of the inelastic energy loss to show that it has a strong effect on the dynamic motion of slip on the fault. Some examples of the solutions are illustrated in Fig. 1. It is concluded that the backward slip is hardly possible as far as the slip motion is resisted by frictions, that the final displacement in the solutions exceeds the value expected from the static solution. The stress drop is consequently larger than the effective stress, the difference between the initial stress and the dynamic fricional stress. It is seen that slip continues after the crack expansion stops. It has been pointed out that this is a remarkable feature of the dynamic process of fracturing. Our model is two-dimensional, however, by the following discussion, it is considered that the solutions are applicable to the three-dimensional source function.

The static solution of the two-dimensional antiplane strain shear crack under the

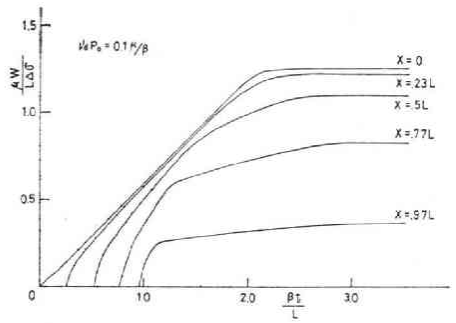

Fig. 1 (a)

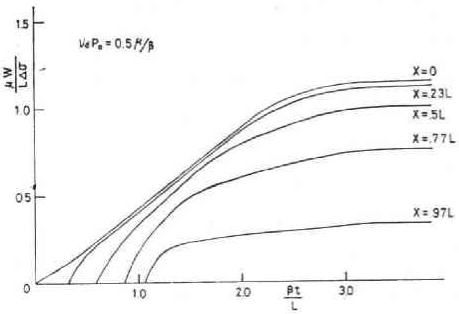

Fig. 1 (b)

Fig. 1. Examples of the temporal and spatial variations of the displacement on the antiplane strain shear cracks in the presence of the frictions involving (a) weakly and (b) strongly viscous terms obtained in the previous paper.

uniform shear stress σ is given by

$$w_s = \frac{\sigma}{\mu}(L^2-x^2)^{1/2} \tag{1}$$

where L is the half of the crack length, μ the rigidity of the medium, and x the co-ordinate of a point on the crack measured from the centre of the crack. The spatial variation of the final displacement on the crack in the dynamic solution previously obtained is well approximated as the same form as the static solution:

$$w_f = K\frac{\sigma_e^0}{\mu}(L^2-x^2)^{1/2} \tag{2}$$

where σ_e^0 is the difference between the initial stress and the dynamic frictional stress, K the constant depending upon the value of the viscous friction. On the other hand, the static solution of the three-dimensional circular shear crack is represented as

$$w_c = \frac{12}{7\pi}\frac{\sigma}{\mu}(R^2-\rho^2)^{1/2} \tag{3}$$

where R is the radius of the crack, ρ the distance of a point on the crack from its centre.

Here we note that, letting R correspond to L and ρ to x, the static solution of the cricular shear crack has a similar spatial distribution of displacement to that of the antiplane strain shear crack, but only differs in the amplitude by a factor of $12/7\pi$. On the analogy of similarity between w_f and w_s together with that between w_s and w_c, it is reasonable for the first approximation to expect that the dynamic process of slip on a circular fault is well represented by the dynamic solutions obtained in the previous paper. On the circular crack, the dislocation motion is the mixture of the screw type and the edge type. Burrsige (1973) has given the slef-similar solutions of the edge type cracks in the presence of the frictions but lacking the cohesion. Their solutions show the similarity of the spatial variations of slip to our solutions while the crack expansion

is in progress for the same range of the rupture velocity. Burridge suggests, furthermore, that it is more likely for the fault to expand in a circular shape than in an elliposidal shape. In actual, at an earthquake focus, it may be difficult to imagine that the fault keeps on expanding in a circular shape to a long radius. As concerns the small earthquakes with small dimensions, however, the shape of the fault will be approximately kept circular. Therefore, our applciation of the two-dimensional solutions to the three-dimensional source time function on a circular fault is considered to be reasonable, and the source time function thus specified to be representative of the dynamic motion of slip on a circular fault.

Let w denote the two-dimensional solution of the dynamic fracture problem obtained in a previous paper. Then the source time function in our study is given by, letting ρ correspond to x,

$$D(\rho,t) = \frac{24}{7\pi} w(\rho,t) \tag{4}$$

The value of D only depends upon the radius ρ and time t.

3. Far-field radiation of the seismic waves

We consider an infinite elastic medium, which is supposed isotropic and homogeneous, with a fault surface at $y=0$. The rupture starts at the origin of the coordinate system (x, y, z), and the crack expands in a circular shape to its maximum radius R. The direction of relative slipping is taken to be parallel to the positive z-axis. Here we introduce a polar coordinate system (r, θ, ϕ) by the relations

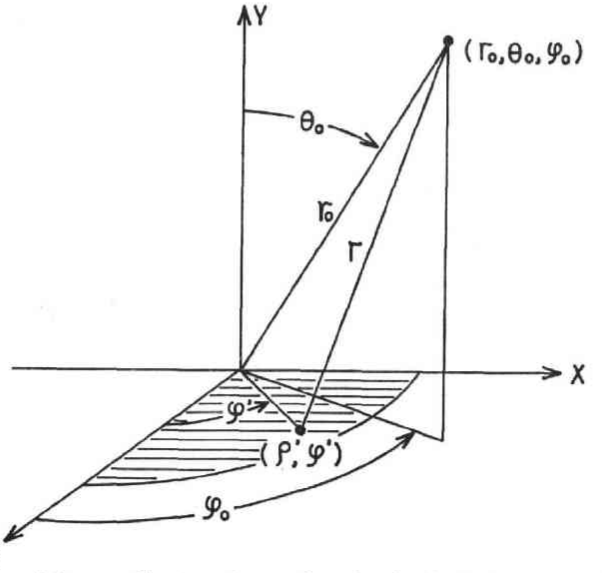

Fig. 2. Configuration of the coordinate systems referred to in the text. The fault is represented by the hatched area.

$$x = r \sin\theta \sin\phi$$
$$y = r \cos\theta \tag{5}$$
$$z = r \sin\theta \cos\phi$$

We specify the point on the fault by $(\rho'\ \phi')$, and the observation point by $(r_0,\ \theta_0,\ \phi_0)$. r_0 is the distance of the observation point from the centre of the crack (Fig. 2).

Following Haskell, the displacement components of P and S waves at a remote point from the source region is represented in the form of surface intergral of the source function:

$$U_r^p = \frac{24}{7\pi}\frac{1}{4\pi\beta r_0}\left(\frac{\beta}{\alpha}\right)^3 \sin 2\theta_0 \cos\phi_0 I_\alpha$$
$$U_\theta^s = \frac{24}{7\pi}\frac{1}{4\pi\beta r_0}\cos 2\theta_0 \cos\phi_0 I_\beta \tag{6}$$
$$U_\phi^s = \frac{24}{7\pi}\frac{1}{4\pi\beta r_0}\cos\theta_0 \sin\phi_0 I_\beta$$

where the subscripts r, θ, and ϕ are used to indicate the r, θ, and ϕ components of displacement, the superscripts p and s to indicate the displacements due to P and S waves, respectively. $I_{\alpha,\beta}=\int \dot{w}\left(\rho', t-\frac{r}{\alpha,\beta}\right)dS$, dS being the surface element on the fault, α, β the propagation velocity of P and S waves, respectively. r is the distance form a point on the fault surface to the observation point, approximated as $r=r_0-\rho \sin\theta_0 \cos(\phi_0-\phi')$. The temporal and the spatial variations of the source time function are shown in Fig. 1. The solutions shown in the figures are obtained numerically, that integrations are carried out numerically. The ratio of the P- to the S-wave velocity is assumed to be that of the possion body $\sqrt{3}$ in our calculations.

The examples of the wave form $I_{\alpha,\beta}$ at several angles of θ_0 are shown in Fig. 3 and in Fig. 4 for two cases of the source time function, a weakly viscous soruce shown in Fig. 1(a) and a strongly viscous source shown in Fig. 1 (b), respectively. Time is measured from the onset of displacement both for P and for S waves. The observed displacement pulse should be the correction in the amplitude by the geometrical spreading factor and also by the radiation pattern coefficient. Due to the symmetry of the source time function with respect to angle ϕ', $I_{\alpha,\beta}$ is independent of angle ϕ_0. Since the source time function is much smoothed by the damping effect in the case of the strongly viscous friction compared with in the case of the weakly viscous friction, the pulse shape of either P or S waves is also smoothed in the case of highly viscous source.

At $\theta_0=0$, the P- and the S-wave pulses are identical as in other studies. The value of $I_{\alpha,\beta}$ takes its maximum at $t=1.0L/\beta$, which corresponds to the time when the crack expansion stops. At higher angles of θ_0, two phases are clearly seen on the pulse of either P or S waves (indicated by arrows in the figures), which may be interpreted as

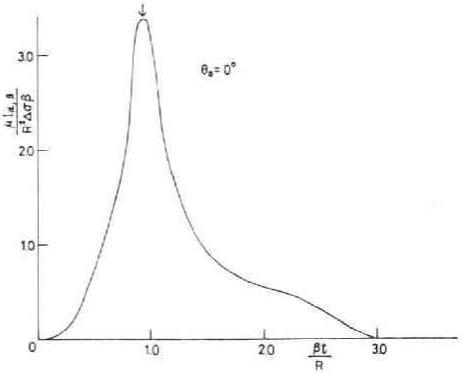

Fig. 3 (a)

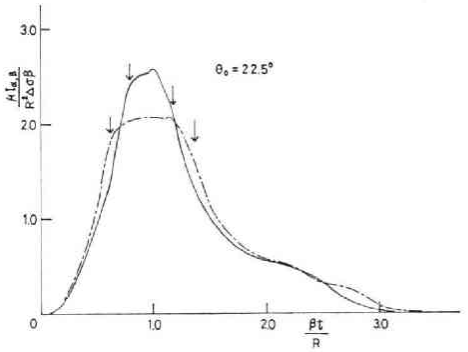

Fig. 3 (b)

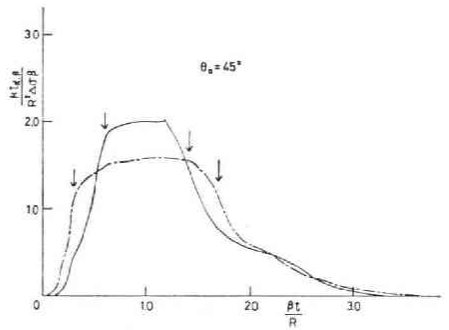

Fig. 3 (c)

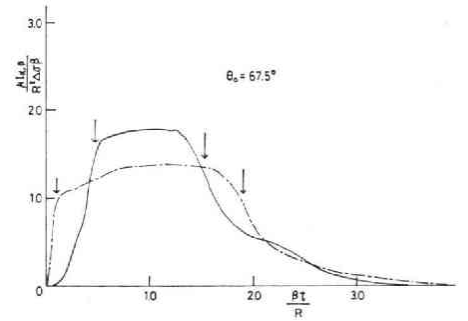

Fig. 3 (d)

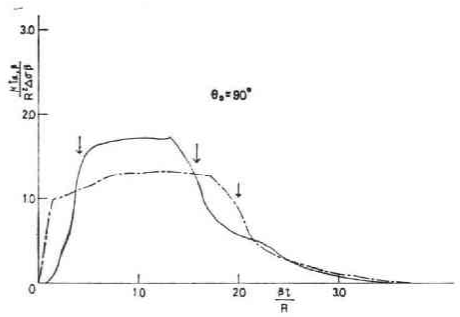

Fig. 3 (e)

Fig. 3. Far-field displacement pulses radiated from a less viscous source of slip, the temporal and spatial variations of which shown in Fig. 1 (a). Solid lines represent the P-wave pulses, and broken lines the S-wave pulses. Examples are shown at several angles θ_0 measured from the normal to the fault. Time is measured relative to the onset of the pulse. The stopping pahses from the nearest and the farthest point on the edge of the fault are clearly seen (indicated by arrows).

the stopping phases corresponding to the nearest and the farthest edges of the crack from the observation point. We also note that the decrease in the amplitude of $I_{\alpha,\beta}$ after the peak value in our model is more gradual than in any other source model. These two remarkable charactersitics of the seismic pulse, appearance of two stopping phases and gradual decrease after the peak, are considered to be attributed to the characteristics of the source time function, the spatial variation of slip motion on the fault and the long duration of slip which continues after the crack expansion stops. The pulse width of the seismic displacement in our model is longer than was predicted

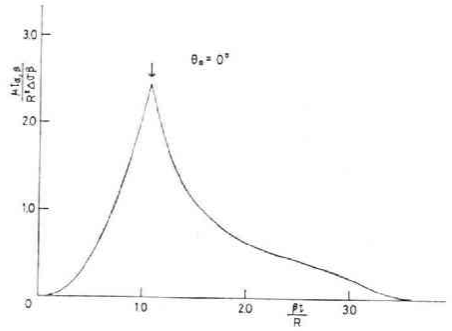

Fig. 4 (a)

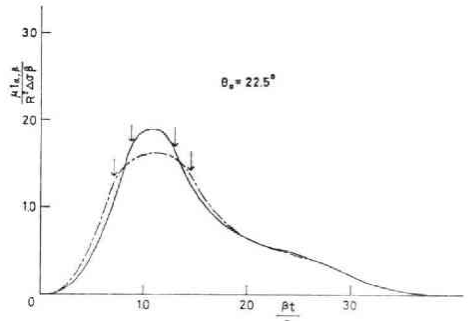

Fig. 4 (b)

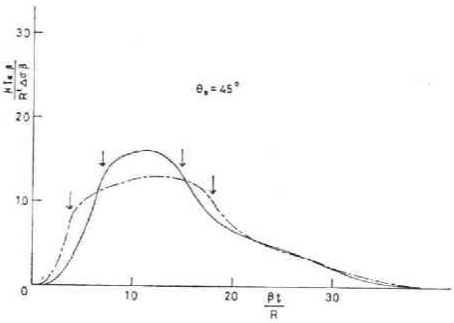

Fig. 4 (c)

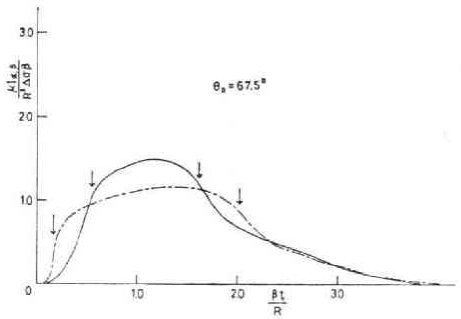

Fig. 4 (d)

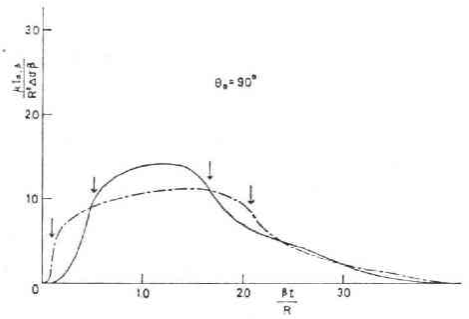

Fig. 4 (e)

Fig. 4. Far-field displacement pulses radiated from a much viscous source of slip, the temporal and spatial variations of which shown in Fig. 1 (b). Solid lines represent the P-wave pulses, and broken lines the S-wave pluses. Exmaples are shown at several angles of θ_0 measured from the normal to the fault. Time is measured relative from the onset of the pulse. The stopping phase from the nearest and the farthest point on the edge ot the fault are seen. The seismic pulses are smoothed by the damping effect of much viscous friction compared with those shown in Fig. 3.

in any other source model.

The effect of the crack propagation appears to increase the predominant period of either the P- or the S-wave displacement pulse with increasing θ_0. The S-wave pulse is more strongly affected by this effect than the P-wave pulse is, so that the predominant period of the S-wave pulse is longer than that of the P-wave pulse at higher

Fig. 5. Far-field displacement spectrum at several angles measured from the normal to the fault radiated from a less viscous source of slip shown in Fig. 1(a). Solid lines represent the P-wave spectra, and the broken lines the S-wave spectra. The corner frequencies of P waves are higher than those of S waves. At high angles, the decay of the S-wave spectra at high frequencies is more gradual than that of the P-wave spectra.

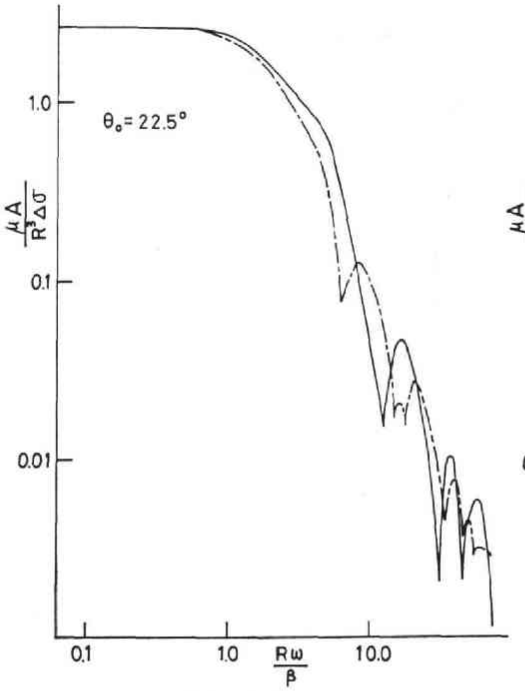

Fig. 5 (a)

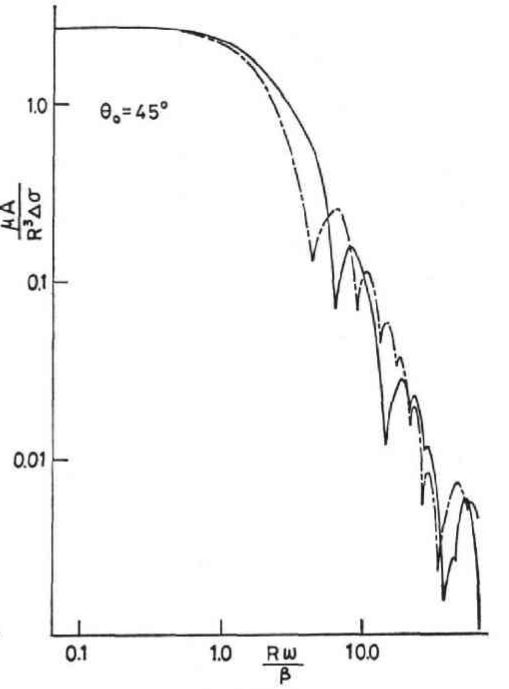

Fig. 5 (b)

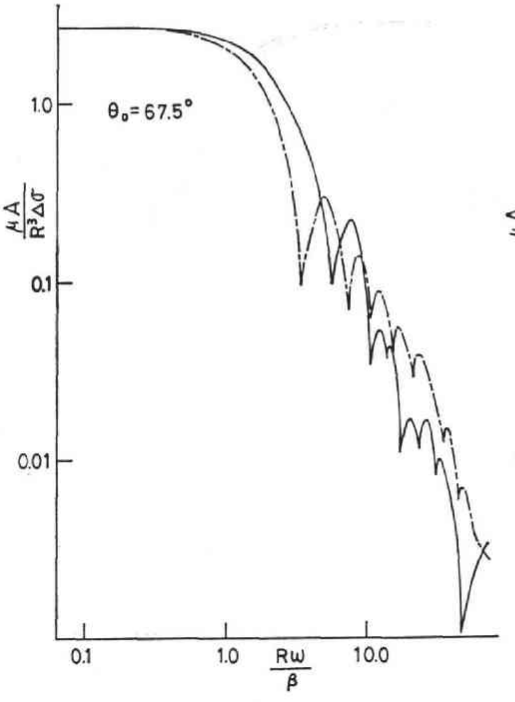

Fig. 5 (c)

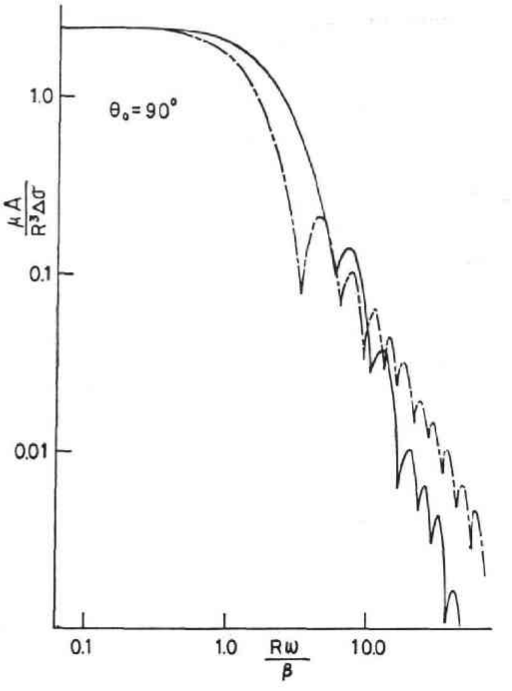

Fig. 5 (d)

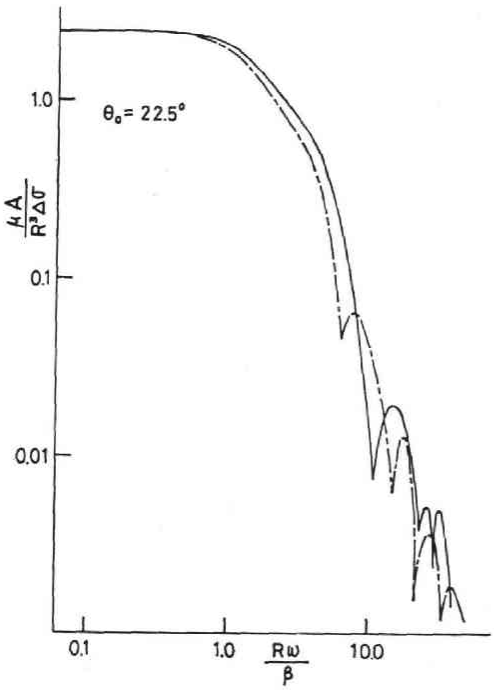

Fig. 6 (a)

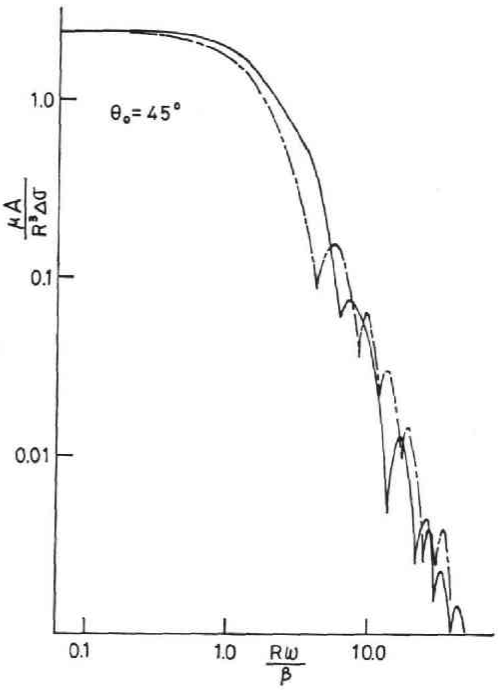

Fig. 6 (b)

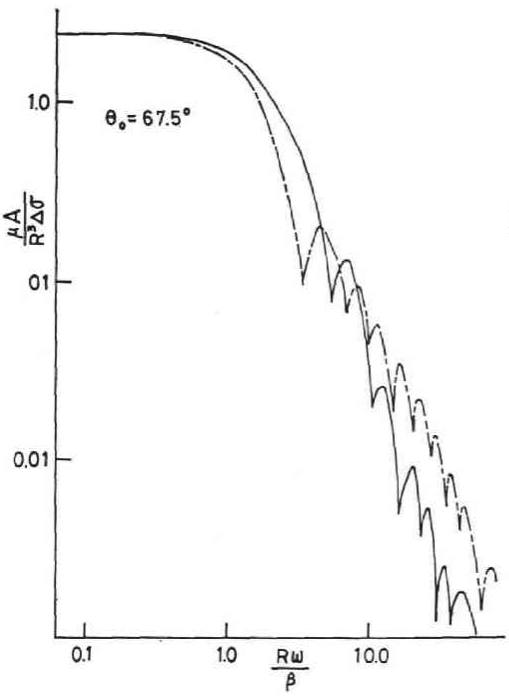

Fig. 6 (c)

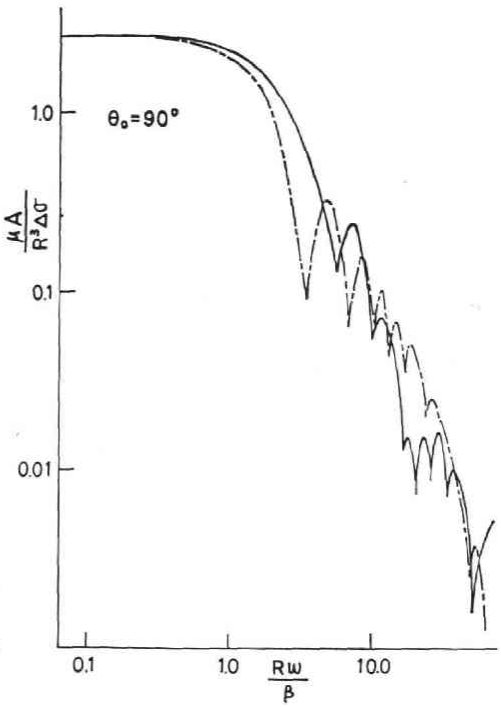

Fig. 6 (d)

angles of θ_0. As the rupture velocity is as fast as the S-wave velocity, the S-wave pulse suffers nearly a step-like onset at angles of θ_0 higher than 45°, while the onset of the P-wave pulse is not so steep.

The Fourier transform of $I_{\alpha,\beta}$ is given by

$$F_{\alpha,\beta}(\omega) = \int_{-\infty}^{\infty} I_{\alpha,\beta}(t) e^{-i\omega t} dt \tag{7}$$

and the spectral amplitude of $I_{\alpha,\beta}$ by

$$A_{\alpha,\beta}(\omega) = |F_{\alpha,\beta}(\omega)| . \tag{8}$$

The spectral amplitudes of $I_{\alpha,\beta}$ appearing in Fig. 3 and in Fig. 4 are shown in Fig. 5 and in Fig. 6 for several angles of θ_0, respectively. The spectral amplitude of the seismic displacement is characterized by the flat level at low frequencies with the decay in high frequencies. The corner frequency is defined as the frequency at which the two trends in low and high frequencies intersect. The values of the corner frequencies of P and S waves at several angles of θ_0 are summarized in Table 1 with the ratios.

Table 1 *Less viscous source* *much viscous source*

θ_0	$f_{c\alpha}'\left(\frac{a}{R}\right)$	$f_{c\beta}'\left(\frac{\beta}{R}\right)$	$f_{c\alpha}/f_{c\beta}$	$f_{c\alpha}'\left(\frac{a}{R}\right)$	$f_{c\beta}'\left(\frac{\beta}{R}\right)$	$f_{c\alpha}/f_{c\beta}$
22.5	0.225	0.303	1.29	0.215	0.285	1.31
45.0	0.176	0.209	1.46	0.174	0.204	1.48
67.5	0.159	0.166	1.66	0.152	0.157	1.68
90.0	0.152	0.158	1.67	0.145	0.151	1.70

The non-dimensional corner frequency of the P-and the S-wave spectra and their ratio as a function of the angle measured from the normal to the fault. The scaling factor used to reduce $f_{c\alpha}$ or $f_{c\beta}$ to a non-dimensional value $f_{c\alpha}'$ or $f_{c\beta}'$ is given in the parenthesis.

It is seen, as is expected from the study of the seismic pulse in the tim domain, that the corner frequencies of P waves are higher than those of S waves, and their difference increases with increasing angle of θ_0. At angles of θ_0 higher than 67.5°, the ratio of the P- to the S-wave corner frequency is nearly 1.70, larger than the values predicted in the previous studies. We note that at higher angles of θ_0, the decay of the S-wave spectra at high frequencies are much gradual compared with that of the P-wave spectra, that is, the S-wave pulse contains more of high frequency components relative to low frequency components than the P-wave pulse does. This is attributed to the steeper onset of the S-wave pulse, the consequence of the high rupture velocity. At θ_0 higher than 67.5°, the P-wave spectrum decreases in inverse proportion to ω^2 beyond the corner frequency, on the other hand, the S-wave spectrum shows the $\omega^{-1.5}$-decay near the corner frequency.

Fig. 6. Far-field displacement spectrum at several angles measured from the normal to the fault radiated from a much viscous source of slip shown in Fig. 1(b). Solid lines represent the P-wave spectra, and the broken lines the S-wave spectra.

Our model relates the source dimension R to the corner frequency as

$$R = \frac{f'_{c\alpha}\alpha}{f_{c\alpha}} \tag{9}$$

or

$$R = \frac{f'_{c\beta}\beta}{f_{c\beta}} \tag{10}$$

Since the value of f_c' for either P or S waves is obtained to be smaller than other models, our model estimates the source dimension at a smaller value, for instance, at 70 pcercent or 50 percent of the value to be estimated according to the model of Sato and Hirasawa or of Brune, respectively.

The stress drop, the difference in the shear stress before and after faulting, is related to the seismic moment M_0 and the source dimension R as

$$\Delta\sigma = K\sigma_c{}^0 = k\frac{M_0}{R^3} \tag{11}$$

where k=0.43, independent of the value of the viscous friction. The coefficient k in (11) is equal to that appearing in the relation given by Keilis-borok (1959). Since the stress drop is in inverse proporition to the cube of R, the estimates of the stress drop is sensitively affected by the estimated value of the source dimension. Our model estimates the source dimension at a smaller value, consequently, the stress drop will be estimated larger, 3 or 8 times larger than the value to be estimated according to the model of Sato and Hirasawa or of Brune, respectively.

4. Discussions

The far-field seismic radiations from circular faults are studied in detail in order to see the effect of the dynamic features of the fracturing process on them. The fault geometry employed in our model is simple. The fault geometry has an effect on the characteristics of seismic radiations. Comparison of our results together with those by Sato and Hirasawa (1973), both of which are for circular faults, with the results by Savage (1972) for a long thin fault model of Haskell (1964) may visualize the effect of the fault geometry. In the latter case, the fault has two different characteristic dimensions, the length and the width. The corner frequency of the spectrum is controlled by the fault length rather than the fault width which on the other hand determines the rise time and the amount of slip. For a circular fault, the corner frequency, the rise time, and the amount of slip are mutually related through only one characteristic length, the radius of the fault. A long thin fault model predicts that the P- wave corner frequencies are no more than the S-wave corner frequencies on the average (Savage, 1972). Our result shows that the circular fault geometry, on the contrary, results in the systematic shift of the P-wave corner frequencies to higher values than the S-wave corner frequencies. The physical justification of a long thin fault geometry may be expected for earthquakes large enough that the equidimensional

fault growth is arrested by the Earth's surface or by some geological localities. As a model of the fracture process of small earthquakes with small dimensions, however, a circular fault model is considered physically appropriate, at least for a first approximation. Molnar et al. (1973) have summarized the observations of the P- and the S-wave corner frequencies for rather small earthquakes reproted by Hanks and Wyss (1972), Wyss and Hanks (1972), Wyss and Molnar (1972), Molnar and Wyss (1972), and Trifunac (1972), to show that the corner frequencies of P waves are systematically larger than the S-wave corner frequencies, which implies that during a small earthquake the fault grows equidimensionally to its final size. The fault size for a small earthquake is represented by only one characteristic length, the radius of the fault.

The characteristics of the seismic radiations are also much dependent upon the dynamic process of slip at the source. Our model predicts that the ratio of the P- to the S-wave corner frequency is about 1.70 at higher angles of θ_0, which is larger than the values predicted in the previous models. This prediction of a large ratio may be interpreted in terms of the pulse widths of P and S waves in the time domain. At higher angles of θ_0, the interference effects due to the finiteness of the fault appear on seismic pulses, especially more intensely on S-wave pulses. Since the rupture velocity is as high as the S-wave velcoity, the S-wave pulse at higher angles of θ_0 experiences a step-like discontinuity at the onset, while the onset of the P-wave pulse is not so steep due to the higher propagation velocity of P waves. Furthermore, as slip at the centre of the crack continues long after the crack stops expanding while near the edge slip is step-like, the far-field displacement pulse has nearly a constant level between two stopping phases from the nearest and the farthest points on the edge of the fault. These effects make the effective width of the S-wave pulse much larger than that of the P-wave pulse. Therefore, the P-wave corner frequency is much higher than the S-wave corner frequency, and the ratio appears higher.

According to Savage (1974), a generalized Haskell model (1964) to a circular fault gives two corner frequencies in the far-field specterum of seismic waves. One is associated with the high-frequency trend and the intermediate-frequency trend, and the other with the intermediate- and low-frequency trend. He showed that the S-wave corner frequencies (associated with the high- and intermeidate-frequency trend) should be larger than the P-wave corner frequencies for most part of the focal sphere, but that the secondary corner frequencies (associated with the intermediate- and low-frequency trned) of the S-wave spectrum may be smaller than the P-wave corner frequencies. He suggested that, since the S-wave corner frequencies may appear very large at some stations, the secondary corner frequencies will be mistaken for the "real" corner frequencies. He interpreted the demonstration by Molnar et al. (1973), that the P-wave corner frequencies exceed the S-wave corner frequencies, as above. Our model, however, clearly shows that the P-wave corner frequencies exceed the S-wave corner frequencies for most part of the focal sphere. The conrer frequency in our determination is associated with the high-frequency trend, but not with the intermediate-frequency trend. This discrepancy may be attributed to the difference in

the source time functions specified in two models. The soruce time function specified in the Haskell fault model may be somewhat unrealistic and not applicable to a circular fault. For a long thin fault, the source time function in Haskell model may be valid in the physical sense, but for a circular fault, a simple function may not be repreesentative of the fault slip. Our model specifies the source time function as a solution to the physical conditions on the fault, and therefore accounts for the dynamic features of slip on the fault.

The dynamic features of slip at the source is found to have an effect also on the relation between the corner frequency and the source dimension. Our model relates the source dimension to the corner frequency of the P- or the S-wave spectrum as is given by (9) or (10). The dimensionless values $f_{c\alpha}'$ and $f_{c\beta}'$ are obtained smaller in our study than in the previous studies, so that the source dimension will be estimated at a smaller value than to be estimated according to other models. A smaller estimate of the source dimension is a consequent result from the dynamic feature of the fracture process at the source that slip continues even after the fault stops expanding. The rise time of the particle at the centre of the fault, for instance, is obtained about two times longer than the time needed for the fault to expand to its final size. The longer duration of slip than the time needed for the fault expansion causes the predominant period of the radiated waves to be longer than the value $2R/V_r$, which may be expected from a simple consideration. A kinematic model, which simply assumes the soruce time function on the basis of some physical considerations rather than specifies it as a dynamic solution to certain stress conditions, has never accounted for this dynamic feature of slip on the fault. Our model, which accounts for this dynamic feature of slip, leads to a smaller estimate of the source dimension, which in turn results in a larger estimate of the strees drop.

It is an important problem to estimate the stress drop associated with an earthquake. For the reasonable estimates of the stress drop, it is required that the source dimensions must be properly estimated. Our study suggests that for the proper estimates of the source dimensions, and consequently of the stress drop, the model used should be such that the source time function is specified as a result of a certain physical process at the source.

Acknowledgements: We are indebted to Professor Z. Suzuki for his helpful advices throughout this study. We express our hearty thanks to Professor T. Hirasawa for reading the manuscript critically and providing many invaluable comments and suggestions. Discussions with Dr. H. Hamaguchi, Mr. K. Yamamoto, and Mr. T. Sato have been very helpful. Many thanks are due to all the staffs of Seismological Observatories of Tohoku University.

References

Aki, K., 1968: Seismic displacements near a fault, J. Geophys. Res., **73**, 5359–5376.

Archambeau, C., 1968: General theroty of elastodynamic source field, Rev. Geophys., **6**, 241–288.

Brune, J.N., 1970: Tectonic stress and the spectra of seismic shear waves from earthquakes, J. Geophys. Res., **75**, 4977–5009.

Brune, J.N. and C.R. Allen, 1967: A low stress-drop, low mangitude earthquake with surface faulting: The Imperial, California, earthquake of March 4, 1966, Bull. Seism. Soc. Amer., **57**, 501–514.

Burridge, R., 1969: The numerical solution of certain integral equations with non-integrable kernels arising in the theory of crack propagation and elastic wave diffraction, Phil. Trans. Roy. Soc. London, **265**, 353–381.

Burrdige, R., 1973: Admissible speeds for plane-strain selfsimilar shear carcks with friction but lacking cohesion, Geophys. J.R. astr. Soc., **35**, 439–455.

Burrdige, R., 1975: The effect of sonic rupture velocity on the ratio of S to P corner frequencies, Bull. Seism. Soc. Amer., **65**, 667–675.

Dahlen, F.A., 1974: On the ratio of P-wave to S-wave corner frequencies for shallow earthquake sources, Bull. Seism. Soc. Amer., **64**, 1159–1180.

Haskell, N.A., 1964: Total energy and energy spectral density of elastic wave radiation from propagating faults, Bull. Seism. Soc. Amer., **54**, 1181–1841.

Haskell, N.A., 1969: Elastic displacements in the near-field of a propagating fault, Bull. Seism. Soc. Amer., **59**, 865–908.

Hanks, T.C. and M. Wyss, 1972: The use of body-wave spectra in the determination of seismic-source parameters, Bull. Seism. Soc. Amer., **62**, 561–589.

Izutani, Y., 1974: Source parameters of some shallow earthquakes as derived from body waves, Master Thesis, Tohoku Univ.

Keilis-Borok, V.I., 1959: On estimation of the displacement in an earthquake source and of source dimensions, Ann. Geofis. (Rome) **12**, 205–214.

Madariaga, R., 1976: Dynamics of an expanding circular fault, Bull. Seism. Soc. Amer., **66**, 639–666.

Masuda, T., S. Horiuchi, and A. Takagi, 1977: Dynamic features of expanding shear cracks in the presence of frictions, Sci. Rep. Tohoku Univ., Ser. 5,

Molnar, P. and M. Wyss, 1972: Moments, source dimensions and stress drop of shallow focus earthquakes in the Tonga-Kermadec Arc, Phys. Earth Planet Int., **6**, 263–278.

Molner, P., B. E. Tucker, and J.N. Brune, 1973: Corner frequencies of P and S waves and and models of earthquake sources, Bull. Siesm. Soc. Amer., **63**, 2091–2104.

Sato, T. and T. Hirasawa, 1973: Body wave spectra from propagating shear cracks, J. Phys Earth, **21**, 415–431.

Savage, J.C., 1966: Radiation from a realistic model of faulting, Bull. Seism. Soc. Amer., **56**, 577–592.

Savage, J.C., 1972: Relation of corner frequency to fault dimensions, J. Geophys. Res., **77**, 3788–3795.

Savage, J.C., 1974: Relation between P- and S-wave corner frequencies in the seismic spectrum, Bull. Seism. Soc. Amer., **64**, 1621–1627.

Thatcher, W. and T.C. Hanks, 1973: Source parameters of Southern California earthquakes, J. Geophys. Res., **78**, 8547–8576.

Trifunac, M.D., 1972: Stress estimates for the San Fernando, California, earthquake of February 9, 1971, Bull. Seism. Soc. Amer., **62**, 721–750.

Wyss, M. and J.N. Brune, 1968: Seismic moment, stress, and source dimensions for earthquakes in the California-Nevada region, J. Geophys. Res., **73**, 4681–4694.

Wyss, M. and T.C. Hanks, 1972: The source parameters of the San Fernando earthquake (February 9, 1971) inferred from teleseismic body waves, Bull. Seism. Soc. Amer., **62**, 591–602.

Wyss, M. and P. Molnar, 1972: Source parameters of intermediate and deep focus earthquakes in the Tonga Arc, Phys. Earth Planet. Int., **6**, 279–292.